

Supplementary Figures

GATA4-driven miR-206-3p signatures control orofacial bone development by regulating osteogenic and osteoclastic activity

Shuyu Guo^{2,3,4*}, Jiawen Gu^{3,4*}, Junqing Ma^{2,3,4*}, Rongyao Xu^{3,4}, Li Meng^{3,4}, Haojie Liu^{3,4}, Qingheng Wu^{3,4}, Lu Li^{1,3,4} & Yan Xu^{1,3,4} 

¹ Department of Periodontology, The Affiliated Stomatological Hospital of Nanjing Medical University, Nanjing, China.

² Department of Orthodontics, The Affiliated Stomatological Hospital of Nanjing Medical University, Nanjing, China.

³ Jiangsu Key Laboratory of Oral Diseases, Nanjing Medical University, 140 Hanzhong Road, Nanjing 210029, China.

⁴ Jiangsu Province Engineering Research Center of Stomatological Translational Medicine, Nanjing, China.

*These authors contributed equally to this work.

 Correspondence author: Yan Xu, Nanjing Medical University, 140 Hanzhong Road, Nanjing 210029, China. E-mail: yanxu@njmu.edu.cn, Fax: 0086-25-85031976

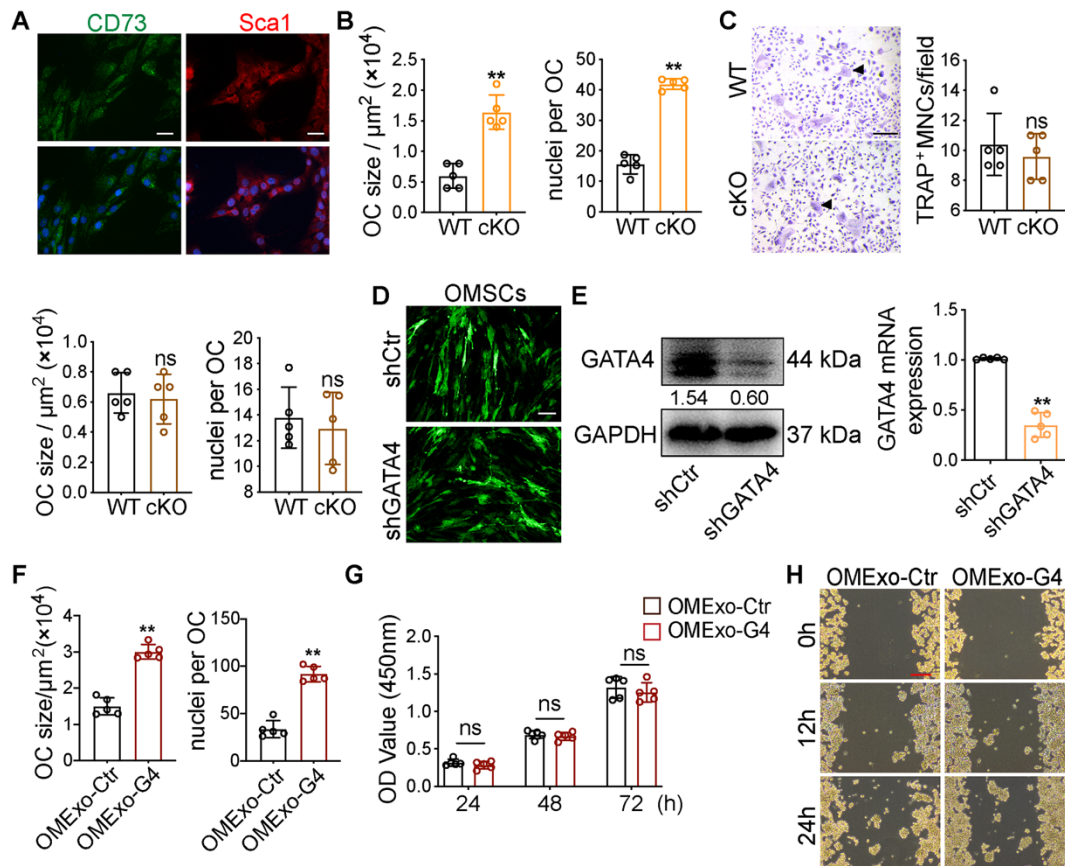


Figure S1. Exosomes derived from OMSCs promote osteoclastic differentiation and function.

(A) Images of OMSCs stained with DAPI to identify nuclei, and immunostained for the mesenchymal stem cell-associated markers (CD73 and SCA1). Scale bar: 200 μm .

(B) The size and the nuclei numbers of TRAP-positive multinucleated cells (TRAP⁺MNCs) in Figure 2A were measured (n = 5). (C) M-CSF and RANKL treated bone marrow-derived macrophages (BMMs) from *Gata4^{fl/fl}* (WT) mice and

Wnt1-cre;Gata4^{fl/fl} (cKO) mice, and then the cells were stained for TRAP. The size and the nuclei numbers of TRAP⁺MNCs were measured (n = 5). Scale bar: 200 μm .

(D) OMSCs infected with lentivirus was assessed by fluorescence microscopy. Scale

bar: 200 μm . (E) Efficiency of GATA4 knockdown in the protein and mRNA level after infection with lentivirus and quantitative analysis of western blotting and

qRT-PCR analysis (n = 5). (F) The size and the nuclei numbers of TRAP⁺MNCs in Figure 2G were measured (n = 5). (G) RAW264.7 cells were cultured in a medium with exosomes isolated from shCtr or shGATA4 OMSCs (OMExo-Ctr, OMExo-G4). After 24 h, cell viability was measured by CCK-8 assay (n = 5). (H) RAW264.7 cells were cultured in osteoclastogenic medium in the presence of OMExo-Ctr or OMExo-G4. Cell mobility was measured by wound healing assay. Scale bar: 200 μ m. Two-tailed Student's t test. Each experiment was repeated at least three times with the same conditions. Data are shown as mean \pm SD. **P < 0.01; ns, not significant.

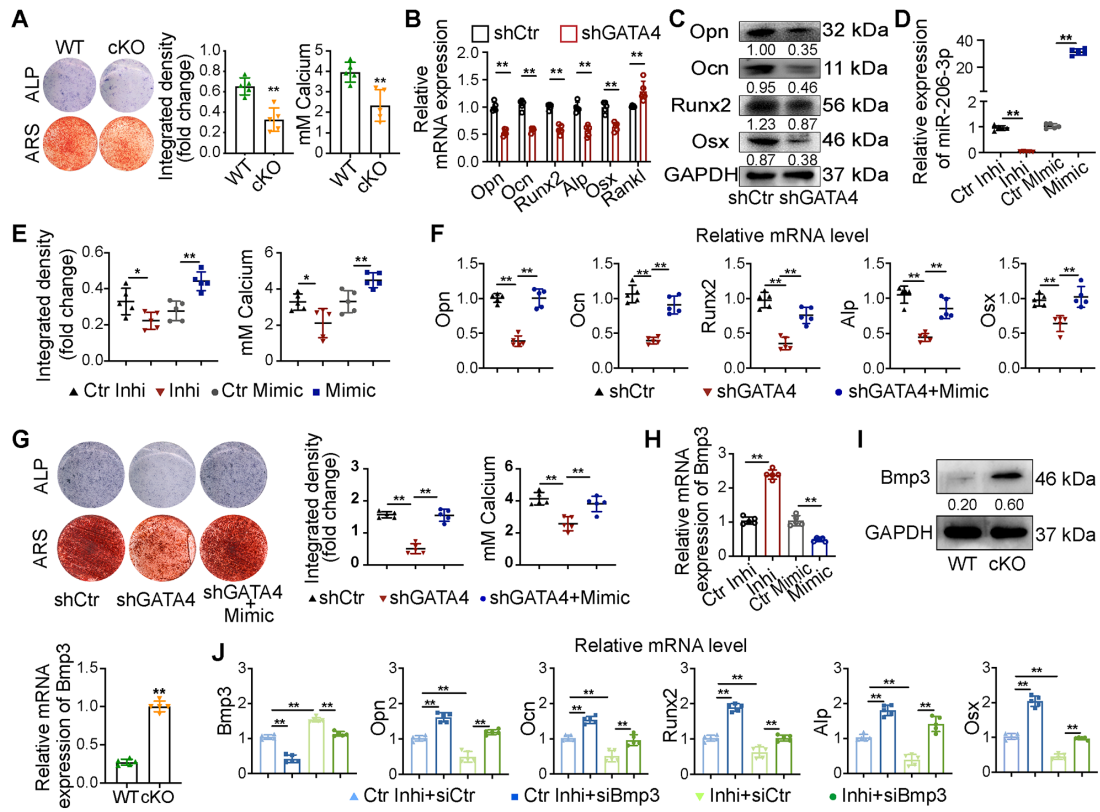


Figure S2. GATA4-miR-206-3p-Bmp3 signaling in regulating osteogenic differentiation of OMSCs.

(A) The ALP activity and the number of mineral nodules of OMSCs from *Gata4*^{fl/fl} (WT) mice or *Wnt1-cre;Gata4*^{fl/fl} (cKO) mice were accessed by ALP and ARS assay (n = 5). Two-tailed Student's t test. (B) Indicated osteogenic gene expression analysis of shGATA4-transfected OMSCs as compared with shCtr OMSCs after 5 days following mineralization induction (n = 5). Two-tailed Student's t test. (C) Protein expression levels of several osteogenic markers in shGATA4-transfected OMSCs were detected by western blotting as compared with shCtr OMSCs after 5 days following mineralization induction (n = 5). Two-tailed Student's t test. (D) qRT-PCR analysis showed the knockdown and over expression efficiency of miR-206-3p in OMSC-derived osteoblasts (n = 5). Ordinary one-way ANOVA. (E) The ALP activity

and semi-quantitative estimation of calcium from Figure 4A were measured (n = 5). Ordinary one-way ANOVA. (F) OMSCs were co-transfected with shGATA4 and miR-206-3p mimic, the mRNA levels of *Opn*, *Ocn*, *Runx2*, *Alp* and *Osx* in the indicated cells were detected using qRT-PCR analysis (n = 5), and (G) ALP and ARS staining to detect osteogenic induction (n = 5). Ordinary one-way ANOVA. (H) miR-206-3p control inhibitor /inhibitor/ control mimic/ mimic transfected OMSCs were subjected to qRT-PCR analysis to detect the mRNA levels of *Bmp3* (n = 5). Ordinary one-way ANOVA. (I) Protein and mRNA levels of *Bmp3* from OMSCs of WT and cKO mice were examined by using western blotting and qRT-PCR analysis (n = 5). Two-tailed Student's t test. (J) OMSCs were co-transfected with miR-206-3p inhibitor and siBmp3, the mRNA levels of *Bmp3*, *Opn*, *Ocn*, *Runx2*, *Alp* and *Osx* in the indicated cells were detected using qRT-PCR analysis (n = 5). Ordinary one-way ANOVA. control inhibitor, Ctr-inhi; inhibitor, inhi; control mimic, Ctr-mimic. Each experiment was repeated at least three times with the same conditions. Data are shown as mean \pm SD. * P < 0.05, ** P < 0.01.

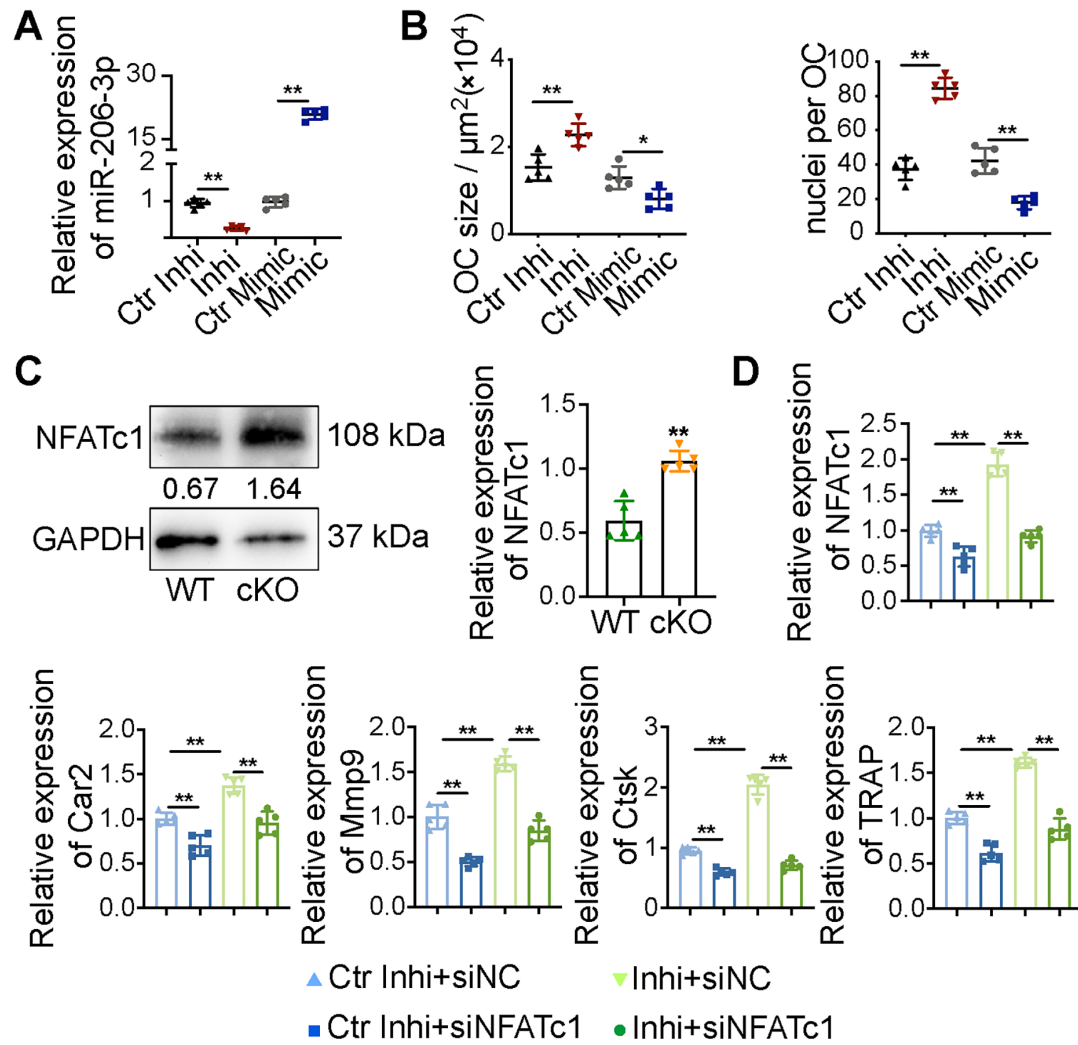


Figure S3. Exosomal miR-206-3p from OMSCs regulates osteoclast activity by targeting NFATc1.

(A) The exosomes from OMSCs were treated with miR-206-3p inhibitor or mimic, respectively, and then co-cultured with RANKL-treated RAW264.7 cells. The knockdown and over expression efficiency of miR-206-3p in osteoclasts was examined by qRT-PCR (n = 5). Ordinary one-way ANOVA. (B) The size and the nuclei numbers of TRAP-positive multinucleated cells (TRAP⁺MNCs) in Figure 5A were measured (n = 5). Ordinary one-way ANOVA. (C) Protein and mRNA levels of NFATc1 of bone marrow-derived macrophages (BMMs) from *Gata4*^{fl/fl} (WT) mice or

Wnt1-cre;Gata4^{fl/fl} (cKO) mice were examined by using western blotting and qRT-PCR analysis (n = 5). Two-tailed Student's t test. (D) RANKL-treated RAW264.7 cells were co-transfected with miR-206-3p inhibitor and siNFATc1, mRNA levels of osteoclast related genes including NFATc1, Car2, Mmp9, Ctsk and TRAP were determined by using qRT-PCR assay. Ordinary one-way ANOVA. Each experiment was repeated at least three times with the same conditions. control inhibitor, Ctr-inhi; inhibitor, inhi; control mimic, Ctr-mimic. Data are shown as mean \pm SD. *P < 0.05, **P < 0.01.

Table S1. Primers used

Gene	Primer	Sequence (5'-3')
NFATc1	Forward	CGAGTTCACATCCCACAG
	Reverse	GACAGCACCATCTTCTTCC
Car2	Forward	ATCCTTGCTCCCTTCTTC
	Reverse	ATCCAGGTCACACATTCC
Mmp9	Forward	TCACTTTCCCTTCACCTTC
	Reverse	ATTGCCGTCCTTATCGT
Ctsk	Forward	CCCATCTCTGTGTCCATC
	Reverse	AGTGCTTGCTTCCCTTCT
TRAP	Forward	CAGCAGCCAAGGAGGACTAC
	Reverse	ACATAGCCCACACCGTTCTC
Opn	Forward	ACCATGCAGAGAGCGAGGATT
	Reverse	GGGACATCGACTGTAGGGACG
Ocn	Forward	ACTCTTGCCTCGTCCACT
	Reverse	GGTCTCTTCACTACCTCGCT
Runx2	Forward	AGTTCCCAAGCTTTCATC
	Reverse	GGCAGGTAGGTGTGGTAGT
Alp	Forward	CAGTGCGGTTCCAGACATAGT
	Reverse	GAACAGAACTGATGTGGAATACG
Osx	Forward	CTACCCATCTGACTTTGCTC
	Reverse	CACTATTTCCCACTGCCTT
Rankl	Forward	AACAGGCCTTTCAA GGAGCTGTGC
	Reverse	AAGAGGACAGACTCACTTTATGGGG
Bmp3	Forward	AACGATGCTGCCATTCT
	Reverse	CTTCCTCCTCTCAACCGA
GAPDH	Forward	GAAGGTGAAGGTCGGAGTC
	Reverse	GAGATGGTGATGGGATTTC

Table S2. Differential genes

Upregulated miRNAs		Downregulated miRNAs
miR-6908-5p	miR-409-3p	miR-206-3p
miR-711	miR-6970-5p	miR-195a-3p
miR-6366	mir-5126	miR-466j
miR-2137	miR-6987-5p	miR-1187
miR-6349	miR-7081-5p	miR-466f
miR-7003-5p	miR-221-3p	miR-669e-5p
miR-99b-5p	miR-652-3p	miR-669f-5p
miR-8101	miR-1981-5p	miR-466m-5p
miR-145a-5p	miR-8119	miR-669m-5p
miR-674-5p	miR-714	miR-669n
miR-3102-5p.2-5p	miR-7653-5p	miR-669o-5p
miR-7654-3p	miR-5100	miR-665-5p
miR-7046-5p	miR-7684-5p	miR-466c-5p
miR-671-5p		miR-466f-5p
miR-425-5p		miR-16-1-3p
miR-5112		miR-1195
miR-30c-5p		miR-297a-5p
miR-3072-5p		miR-466h-5p
miR-7671-3p		miR-5129-3p
miR-3067-3p		miR-669a-5p
miR-34b-3p		miR-669p-5p
miR-574-3p		miR-669c-5p
miR-1249-5p		miR-574-5p
miR-151-3p		miR-3082-5p
miR-34c-3p		miR-669l-5p
miR-100-5p		mir-1194
miR-28a-3p		
miR-7687-5p		
miR-700-3p		
miR-6239		
miR-193b-3p		
miR-3473f		
miR-3104-5p		
miR-211-3p		
miR-423-5p		
miR-7221-3p		
miR-329-3p		
miR-6368		
miR-504-3p		
miR-222-3p		
miR-6910-5p		